Authigenic carbonate burial within the late Devonian Western Canada Sedimentary Basin and its impact on the global carbon cycle

Sean Gazdewich, Tyler Hauck, and Jon Husson

2024

Geochemistry, Geophysics, Geosystems®

AGU ADVANCING EARTH AND SPACE SCIENCES

RESEARCH ARTICLE
10.1029/2023GC011376

Authigenic Carbonate Burial Within the Late Devonian Western Canada Sedimentary Basin and Its Impact on the Global Carbon Cycle

Sean Gazdewich[1], Tyler Hauck[2], and Jon Husson[1]

[1]School of Earth and Ocean Sciences, University of Victoria, Victoria, BC, Canada, [2]Alberta Geological Survey, Edmonton, AB, Canada

Key Points:

- $CaCO_3$ found in Late Devonian shales has average carbon isotope values similar to Late Devonian shallow marine carbonates
- Weight percent values of inorganic carbon content in Late Devonian shales are low compared to average North American shale
- The mass ratio of organic to inorganic carbon in Late Devonian shales is much higher than average North American shale

Supporting Information:

Supporting Information may be found in the online version of this article.

Correspondence to:

S. Gazdewich,
seangazdewich@gmail.com

Citation:

Gazdewich, S., Hauck, T., & Husson, J. (2024). Authigenic carbonate burial within the Late Devonian Western Canada Sedimentary Basin and its impact on the global carbon cycle. *Geochemistry, Geophysics, Geosystems*, *25*, e2023GC011376. https://doi.org/10.1029/2023GC011376

Received 11 DEC 2023
Accepted 9 FEB 2024
Corrected 30 MAR 2024

This article was corrected on 30 MAR 2024. See the end of the full text for details.

Abstract Stable carbon isotope ratios ($\delta^{13}C$ values) of marine carbonates are widely used to infer the relative burial rates of organic carbon, a source of oxygen to the ocean-atmosphere system. This inference, however, is based on the assumption that ocean-atmospheric carbon is buried either as organic carbon or as marine carbonate minerals. The burial of authigenic carbonate minerals formed within sediments after deposition, with low $\delta^{13}C$ values (i.e., similar to organic carbon), has been proposed to explain high $\delta^{13}C$ values in marine carbonates without the need for high burial fluxes of organic carbon. To test this hypothesis, we focus on the Late Devonian, a time period with both pervasive ocean anoxia and a severe reduction in shallow-water carbonate deposition—conditions hypothesized to promote authigenic carbonate formation. We present sedimentological and geochemical data from limestones and black shales of the Wabamun Group, Besa River and Exshaw formations of the Western Canada Sedimentary Basin. These data are compared to inorganic and organic weight percent measurements of North American shales acquired from the USGS National Geochemical Database ($N = 4{,}437$). Results show that basinal shale lack authigenic carbonate with low $\delta^{13}C$ values and that the mean $\delta^{13}C$ value of carbonate in these shales (−0.3‰) do not differ substantially from mean $\delta^{13}C$ of carbonates in platform carbonates of a similar age (0.6‰). Furthermore, inorganic carbon content in Late Devonian shales (mean weight percent = 0.55%, $N = 54$) is lower than average Phanerozoic North American shale (mean of 1.95%, $N = 4{,}055$). Lastly, organic carbon-to-inorganic carbon ratios (OC:IC) of North American shales are well above 1 (mean = 3.72 for Late Devonian shales ($N = 374$), 2.25 for shales ($N = 3{,}653$) of all other ages). Therefore, even if the burial of fine-grained siliciclastic formations carrying authigenic carbonates were to increase, the concomitant increase in organic carbon burial would be even larger. Together, data from this study do not provide evidence that the burial of authigenic carbonate would have a significant effect on global carbon isotope mass balance.

Plain Language Summary Stable carbon isotope ratios ($\delta^{13}C$) of marine carbonate rocks are widely used as a proxy for estimating the relative amount of organic carbon buried throughout geological time. Certain instances in the geologic record indicate pronounced $\delta^{13}C$ excursions for which there is no corroborating evidence for enhanced organic carbon burial. It has been proposed that these excursions may be the result of high burial rates of authigenic carbonate—carbonate minerals formed in situ within marine sediments. We test this hypothesis by analyzing the stable carbon isotope composition of Late Devonian limestones and shales of the Western Canada Sedimentary Basin. We also compare the organic and inorganic carbon compositions of shales from this field study with those from the USGS Geochemical database, an archive of North American shale geochemistry data from across the Phanerozoic. Results show that carbonates found in Devonian shales do not have low average $\delta^{13}C$ values, and average organic carbon content was shown to be significantly higher than inorganic carbon in shale samples across the Phanerozoic. These results signify that authigenic carbonate burial had a negligible effect on the global carbon cycle, and furthermore, an increase in shale burial would result in a higher increase in organic carbon compared to authigenic carbonate.

1. Introduction

Ancient shallow-water carbonates are archives that record the history of Earth's climate and environment. These records are especially useful when investigating events in deep time, such as the Precambrian and the Paleozoic Era, for which there is no deep seafloor record (Müller et al., 1997). Ratios of stable carbon isotopes ($\delta^{13}C$ values) in shallow-water carbonates are used as proxies to interpret the mass fluxes of carbon from the surface

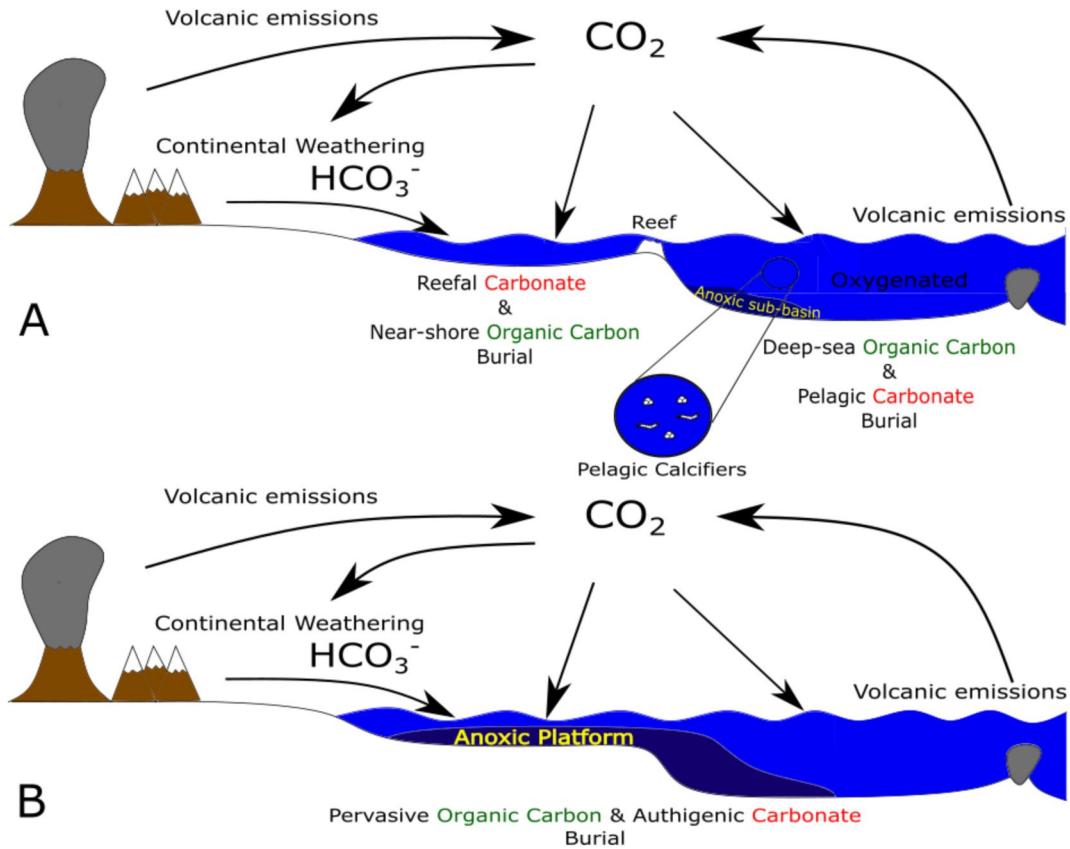

Figure 1. (a) Simplified schematic of the modern carbon cycle. Note that organic carbon is also buried in appreciable amounts in the near shore environment along with calcium carbonate and pelagic calcifiers represent a significant flux of calcium carbonate to the deep ocean crust (Milliman, 1993). (b) Simplified schematic of the Late Devonian carbon cycle. Significant differences between the Late Devonian and the modern include pervasive marine anoxia, the transgression of black shale depositional environments onto carbonate platforms (Savoy et al., 1999; Smith & Bustin, 2000), and the absence of pelagic calcifiers.

environment into sedimentary reservoirs (Ripperdan, 2001), and as a parameter for constraining Earth system models (Berner & Kothavala, 2001; Kump & Arthur, 1999) (Figure 1). When global signals are presumed to be found, profiles of $\delta^{13}C$ values have also been used as a tool for global chronostratigraphic correlation, especially for time periods that lack index fossils (Hay et al., 2019; Knoll et al., 1986). However, recent research has called into question the common framework for interpreting stable carbon isotope records, postulating that a combination of local biogeochemical and diagenetic processes can decouple the chemistry of carbonate sediments from that of the global ocean (Dyer et al., 2015; Fantle et al., 2020; Geyman & Maloof, 2019; Jones et al., 2020; Oehlert & Swart, 2014).

One problem of particular interest is how to explain the large variability in $\delta^{13}C$ values found in Precambrian carbonates (Grotzinger et al., 2011; Halverson et al., 2005; Johnston et al., 2012). Prolonged periods where $\delta^{13}C$ values are high (>+5‰), such as in the Neoproterozoic, imply high rates of organic carbon burial and associated oxygen flux to the ocean-atmosphere system (Kump & Garrels, 1986). This interpretation is difficult to reconcile with other geochemical proxies that indicate low levels of oxygen at this time (Derry, 2015) unless high production of oxygen in the Neoproterozoic is accompanied by high rates of oxidative weathering of the continents or an increase in mantle-derived reductants (Catling & Claire, 2005).

To explain this apparent inconsistency between records of $\delta^{13}C$ values and levels of atmospheric oxygen, one proposal is that authigenic carbonate, carbonate minerals precipitated within the pore spaces of marine siliciclastic formations during early diagenesis, represents an important third sink for carbon, in addition to organic carbon and marine carbonate precipitated from the water column (Higgins et al., 2009). Under this model, carbonate precipitation occurs in conjunction with anaerobic organic carbon degradation, leading to the burial of

carbonate with low $\delta^{13}C$ values. High burial fluxes of this type of authigenic carbonate would result in an increase in the $\delta^{13}C$ values of the dissolved inorganic carbon (DIC) in the ocean. This signal would then be recorded as positive $\delta^{13}C$ values in platform carbonates. Conversely, negative carbon isotope excursions could be explained by a decrease in the burial flux of authigenic carbonate or by the incorporation of authigenic carbonate within carbonate shelf sediments (Schrag et al., 2013). This authigenic sink, though inhibited by the relatively high amounts of dissolved oxygen in modern seawater, could have been prominent in the more oxygen-poor oceans of the Precambrian and could have reemerged during transient expansions of ocean anoxia observed in the Phanerozoic (Grotzinger & Knoll, 1995; Higgins et al., 2009; Planavsky et al., 2014).

For the modern, efforts have been made to quantify the mass fraction of authigenic carbonate in sediments using data from the International Ocean Drilling Program (IODP) (Bradbury & Turchyn, 2019; Mitnick et al., 2018; Sun & Turchyn, 2014). Based on pore-fluid alkalinity measurements, authigenic carbonate is most common on the margins of ocean basins where organic matter delivery is high, and accounts for at least 10% of global carbon burial (Sun & Turchyn, 2014). However, extrapolation of the sparsely distributed IODP data to a more global assessment of authigenic carbonate concluded that the total flux is smaller than previously estimated (Bradbury & Turchyn, 2019). Moreover, in settings where authigenic carbonate is actively forming, the mass of authigenic carbonate is small relative to marine carbonate (Mitnick et al., 2018) and thus unlikely to significantly alter the bulk carbonate $\delta^{13}C$ value of sediment, with the potential exception of environments that have undergone extensive methane oxidation (because such authigenic carbonate tends to have very low $\delta^{13}C$ values). For studies related to deep time, the mass of authigenic carbonate, and its average $\delta^{13}C$ value, was estimated for the Late Devonian-Early Carboniferous Bakken Formation of North Dakota, a fine-grained siliciclastic formation (Barnes et al., 2020). Though found to be high in abundance (weight percent values of 7%–9%), the authigenic carbonate sampled in this study did not have very low $\delta^{13}C$ values (−3–3‰).

The Late Devonian (382.7–358.9 million years old (Ma.)) is an example of a time period in the Phanerozoic when authigenic carbonate may have played a significant role in the global carbon cycle. Globally, it was marked by a widespread reduction in shelf carbonate systems and accompanying global rise in siliciclastic deposition (Barnes et al., 2020; Kaiser et al., 2016; Peterhänsel et al., 2008; van Loevezijn & Raven, 2017). The presence of positive $\delta^{13}C$ excursions in globally dispersed basins (Cramer et al., 2008; Myrow et al., 2011) and the widespread deposition of organic-rich black shales at the Devonian-Carboniferous boundary, often referred to as the Hangenberg Crisis (Becker et al., 2016; Kaiser et al., 2006), suggest a significant perturbation of the carbon cycle. Supplementary geochemical proxies indicate pervasive global ocean anoxia at this time, including high concentrations of framboidal pyrite in black shales (Barnes et al., 2020; Marynowski et al., 2012; Schieber & Baird, 2001) and trace metal enrichment (Barnes et al., 2020; Riquier et al., 2006; Scott et al., 2017), in particular redox-sensitive elements that accumulate in anoxic sediments (e.g., Mo, U, and V). The crash in shelf carbonates is especially significant because mass balance dictates that if alkalinity is not being buried as marine carbonates, then another alkalinity sink (potentially authigenic carbonate) must compensate to balance the input from chemical weathering. In summary, the Late Devonian, defined by global anoxia and a shift from carbonate to marine siliciclastic deposition, implies boundary conditions conducive to the expansion of an authigenic carbonate sink (Figure 1).

Here, we test the importance of authigenic carbonate on carbon isotope mass balance by quantifying the amount and average $\delta^{13}C$ value of inorganic carbon present in the Exshaw and Besa River formations, both Late Devonian black shale units. These values are compared to $\delta^{13}C$ values from coeval shallow marine carbonate units. By comparing the mean $\delta^{13}C$ value for each depositional environment, we intend to broadly evaluate the effect of authigenic carbonate deposition on carbon isotope mass balance based on data from a single basin. In particular, we consider formations that span the Famennian (372.2–358.9 Ma.), as this will allow us to assess the authigenic carbonate sink hypothesis from when marine carbonate depositional environments first contracted, at the Frasnian-Famennian boundary, to the nadir of this constriction, at the end of the Famennian (Barnes et al., 2020; Kaiser et al., 2016).

2. Geologic Setting

Late Devonian strata are well preserved throughout western Canada, where it forms part of the Western Canada Sedimentary Basin (WCSB), spanning an areal extent of approximately 700,000 km^2 (Figure 2). Famennian stratigraphy within the basin is dominated by the carbonates of the Wabamun Group and its equivalents, which

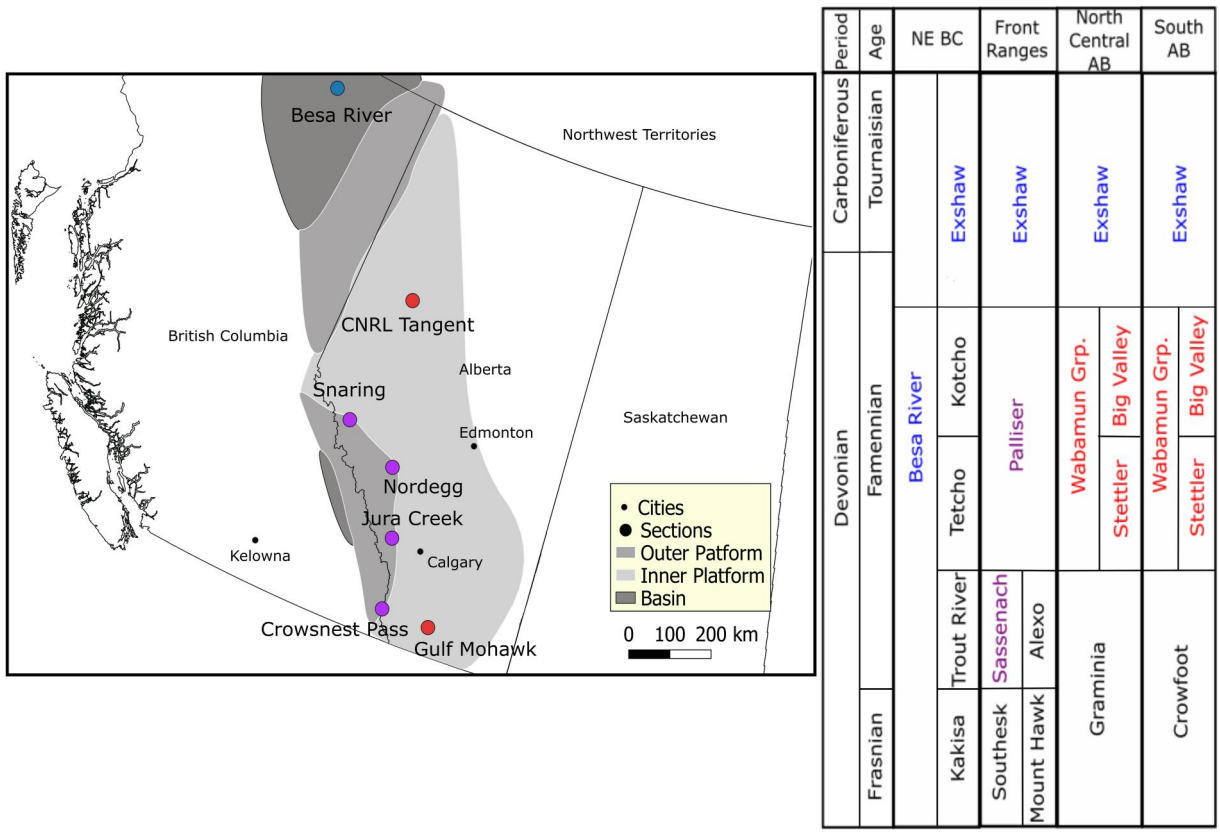

Figure 2. Simplified depositional environments across the WCSB during the Famennian (modified from Peterhänsel et al. (2008)) including sample locations. Each symbol is color coded to reflect its broad depositional environment within the WCSB: deep basin (blue), outer platform (purple) and inner platform (red). Adjacent to the regional map is the Late-Devonian-Early Carboniferous stratigraphy of the WCSB. Stratigraphic nomenclature compiled from de Witt and McLaren (1950), Macqueen and Sandberg (1970), McLaren and Mountjoy (1962), Meijer-Drees et al. (1993), and Richards and Higgins (1988). Studied formations are color coded relative to their depositional environment like in the regional map. Note that the lower member of the Alexo Formation is partly equivalent to the Southesk and Mount Hawk formations (Workum & Hedinger, 1992).

thicken westward (Halbertsma, 1994). Shale and argillaceous limestones are present at the basin margin in the northwest of the WCSB, and platform limestone facies are found in north-central Alberta, which become progressively dolomitic and evaporitic toward the southeast. In Alberta's subsurface, the Wabamun Group comprises the partly dolomitized Stettler Formation, which is interbedded with evaporites in the southeast, and overlain by the open-marine subtidal carbonates of the Big Valley Formation. The peritidal-to-subtidal Palliser Formation, in the Canadian Rockies front ranges to the west, is coeval with the Wabamun Group and overlies the older mixed carbonate-clastic Sassenach Formation (Meijer-Drees et al., 1993; Peterhänsel et al., 2008). Toward the northwest (i.e., northeastern B.C), slope environments are preserved as shales from the Fort Simpson Formation and open-marine carbonates of the Tetcho and Kotcho formations, and the deep basin depositional environment is preserved as marine shales from the Besa River Formation (Ferri et al., 2011).

Toward the end of the Famennian, increased accommodation combined with a nutrient-stressed carbonate system caused the widespread deposition of the organic-rich Exshaw Formation, which covered the entirety of the WCSB and spans the Devonian-Carboniferous boundary (Savoy et al., 1999; Figure 2). The Exshaw is divided into two members: a lower Famennian, laminated shale member, and an upper Tournaisian member comprised of silty to sandy carbonate (Smith & Bustin, 2000).

3. Methods

Seven stratigraphic sections were measured, representing a range of depositional environments. Four outcrop sections were logged in the southern Canadian Rockies: Snaring (53°03′36″N, 118°05′57″W), Nordegg (52° 29′36″N, 116°00′15″W), Jura Creek (51°05′42″N, 115°09′11″W) and Crowsnest Pass (49°37′36″N, 114°38′48″

W). Three cores were logged: A-38-B/94-N-8 Besa River, 09-23-80-24W5 CNRL Tangent and 11-36-7-23W4 Gulf Mohawk, whose geographic locations represent northeast British Colombia, north-central Alberta and southeast Alberta, respectively. These seven sections form a NW to SE transect that is ~1,300 km long (Figure 2). At each locality, the physical stratigraphy was described and lithofacies were correlated with respective formations within the WCSB. Representative samples of each lithofacies were prepared for thin-section petrography. Using standard transmitted microscopy, carbonate lithofacies were classified following Dunham's classification system (Dunham, 1962). During lithostratigraphic logging, samples of siliciclastic mudstone, including mudstone-hosted carbonate concretions, were found, and carbonates were sampled for $\delta^{13}C$ and $\delta^{18}O$ analyses. The sampling resolution was at 0.5–1 m intervals, or at finer resolution on either side of prominent lithologic boundaries. At the University of Victoria, a Dremel drill press was used to extract approximately 10 mg of powder from the finest-grained component of each sample, most often micrite. Aided by thin section analysis, care was taken to avoid sampling late-stage cements such as carbonate veins as well as lithoclast carbonate sediments. For sections 09-23-80-24W5 CNRL Tangent and 11-36-7-23W4 Gulf Mohawk, a Dremel rotary drill with a tungsten carbide cutter bit was used for collecting powder done on site at the Alberta Energy Regulator's Core Research Center in Calgary. Prior to sampling, the external surface of the core was abraded away to minimize the risk of contamination.

A total of 750 samples were measured for $\delta^{13}C$ and $\delta^{18}O$ values, 54 shale/siltstone, and 696 carbonates. Powders were weighed into a glass exetainer and then left to dry in an oven for at least 6 hr at 90°C. Samples were later capped and flushed with helium. The samples then reacted with 15 drops of anhydrous 100% phosphoric acid from a 1 ml syringe. Samples were left to react for 1 hr at 85°C, and CO_2 in the head space was sampled via an auto-sampler and analyzed on a Sercon 20–22 continuous flow isotope ratio mass spectrometer (IRMS) with a Gasbox II front end device at the University of Victoria. All carbon and oxygen isotope ratios are reported in per mil units (‰) relative to the VPDB (Vienna Pee Dee Belemnite) standard. Analytical uncertainty (1σ) is 0.05–0.1‰ for $\delta^{13}C$ and 0.15–0.2‰ for $\delta^{18}O$, based upon replicate measurements of two secondary calcite standards (international standard IAEA-CO-8 and in-house standard VTS).

Powders from 22 shale horizons (out of 54 shale samples total) were measured for their carbonate content (weight percent inorganic carbon). Concretions and carbonate veins were excluded. The carbonate content was measured using a UIC Inc. carbon coulometer with a CM5130 acidification module at the University of Victoria. Between 40 and 70 mg of shale powder was produced, using a rock pulverizer, and was weighed out into vials. A 3 min purge time was used to clear atmospheric CO_2 from the sample vial prior to acid injection. Powder then reacted with 6.5 ml of 2N H_2SO_4. Analysis of each sample was done over 13 min with a frequency of 1 sample measurement per minute. Three "in-house" standards representing a mixture of pure silica sand and pure calcium carbonate at ratios of 90:10, 99:1, and 100:0 were used to calibrate the instrument and for determining precision and accuracy. Because all 22 of these samples were also measured for $\delta^{13}C$ values, coulometry-determined inorganic carbon content was then plotted with respect to IRMS beam area (a function of the amount of CO_2 generated during phosphoric acid digestion and the signal measured on the Faraday cups). A linear fit allowed inorganic carbon content for the remaining 32 shale samples that were measured for $\delta^{13}C$ and $\delta^{18}O$ values to be estimated (Figure S1 in Supporting Information S1). These IRMS-based measurements represent a rough, semi-quantitative estimate for calcium carbonate content.

To aid in the interpretation and discussion of these new data, results are compared with inorganic and organic carbon weight percent measurements (% IC and % OC) from North American marine siliciclastic lithologies (e.g., shales, siltstones, mudstones, and claystones) from the USGS National Geochemical Database (USGS, 2008). These samples have been linked to the North American portion of the Macrostrat database, based upon sample location and its geologic name (Peters et al., 2018), in order to provide age estimates and greater stratigraphic context for the USGS samples. There are a total of 4,027 samples with both % OC and % IC measurements, ranging in age from Precambrian to Cenozoic. Of these data, 382 are from the following Late Devonian-aged formations: Antrim, Chattanooga, Huron, Leatham, New Albany, Ohio, Pilot, Slaven, Three Forks, Vinini, West Range, Woodford, and Woodruff. Several of these formations, however, range younger or older than the Late Devonian (e.g., the New Albany shale Formation extends from the Middle Devonian to the Lower Mississippian).

4. Results

4.1. Lithofacies

4.1.1. Deep Basin—Besa River and Exshaw Formations

Core from A-38-B/94-N-08 Besa River consists of a massive mudrock succession that extends from the Middle Devonian to the Early Carboniferous (Figure 2). A portion of this core was logged and sampled (40 m in length, from 3,985 to 4,022 m below surface), including the contact of the upper Besa River with the lower part of the Exshaw Formation. Because the two formations share similar lithologies, the contact between the two was inferred based on a prior unpublished assessment by CNOOC Petroleum North America ULC. Based on gamma-ray petrophysical logs, this section of the core was recently correlated with the lower Exshaw Formation and the upper Patry Formation, and both of these formations are encapsulated within the newly proposed Besa River Group (Ferri et al., 2021). The bottom 20 m, which represents the Besa River Formation, consists of an alternating succession of laminated and unlaminated (i.e., massive) siltstone. Laminations effervesce in hand sample; however, carbonate minerals are too small to be described in detail in thin section. This succession continues into the Exshaw, however, with more pronounced fissility, and hosts several carbonate concretions (Figure 3a). Pyrite, including as pyrite framboids, is present throughout both formations, forming as lenses or aggregates. The Exshaw Formation is regionally extensive across the WCSB and was observed in this study at four outcrop sections (Nordegg, Jura Creek, Crowsnest Pass) and the two other core sections (Gulf Mohawk and CNRL Tangent). The Exshaw at Jura Creek and Crowsnest Pass also displayed macroscopic carbonate concretions (Figure 3b).

4.1.2. Outer Platform—Sassenach and Palliser Formations

The Sassenach Formation, which underlies the Palliser and is confined to the Jasper sub-basin (Mountjoy, 1980), was sampled and studied at the Snaring section (Figure 2). At this location, the Sassenach is underlain by argillaceaous carbonates and calcareous shales of the Mount Hawk Formation. The basal portion of the Sassenach comprises bioturbated lime mudstone and peloidal-skeletal lime mudstone facies. Large scale soft sediment deformation separates this basal limestone unit from an overlying unit of finely interbedded carbonates-siliciclastics (Figure 3c). The Sassenach is 338 m thick at this locality, and is in conformable contact with the lower Palliser Formation, which marks a transition to subtidal and lower peritidal limestone facies. Portions of the Palliser Formation were sampled from all four field locations, with Jura Creek being the only section that included the whole formation (Kaylor, 1988; Meijer-Drees et al., 1993; Peterhänsel et al., 2008; Richards et al., 1993). The Palliser Formation is further divided into two members:

The Morro member is the lowermost and consists of skeletal lime mudstones and burrowed lime mudstones at its base eventually grading into variably burrowed to skeletal wackestones and packstones. The basal part of the Morro Member can be dolomitic and contain stromatoporoids. The upper portion of the Morro Member features sharp alternations between skeletal packstones, cherty mudstones and burrowed dolostones.

The overlying Costigan Member comprises lime mudstone and laminated microbialites (Figure 3d) (Kaylor, 1988; Peterhänsel et al., 2008), with some cherty horizons found near the top of the Palliser. Laminated microbialites are characteristic of the Costigan but are absent at Nordegg (Figure 2). Here, the identification of the Costigan is based on conodont microfossils (Johnston et al., 2010; Savoy et al., 1999).

4.1.3. Inner Carbonate Platform—Wabamun Group

The Wabamun Group comprises the Stettler Formation and Big Valley Formation, which are recognized broadly in the subsurface (Figure 2). These units underlie the Exshaw Formation. Previous authors have correlated the Wabamun Group to the Palliser Formation, with the Big Valley Formation correlating with the Costigan Member, based on lithological characteristics and conodont fauna (Johnston et al., 2010; Meijer-Drees et al., 1993). At CNRL Tangent, the base of this core (i.e., 1,764–1,788 measured depth (md) in meters) is characterized by recrystallized nodular wackestones (Figure 3f). This facies is conformably overlain by partially dolomitized grainstone and packstone facies representing the Big Valley Formation. This unit, in turn, is overlain unconformably by the lower Exshaw Formation black shale. In the Gulf Mohawk core, there is 7 m of the Stettler Formation, comprised entirely of vuggy nodular oolitic grainstone and laminated microbialite, the lowermost 1.5 m of which is heavily dolomitized (Figure 3e). This unit is overlain by 1 m of skeletal grainstones of the Big

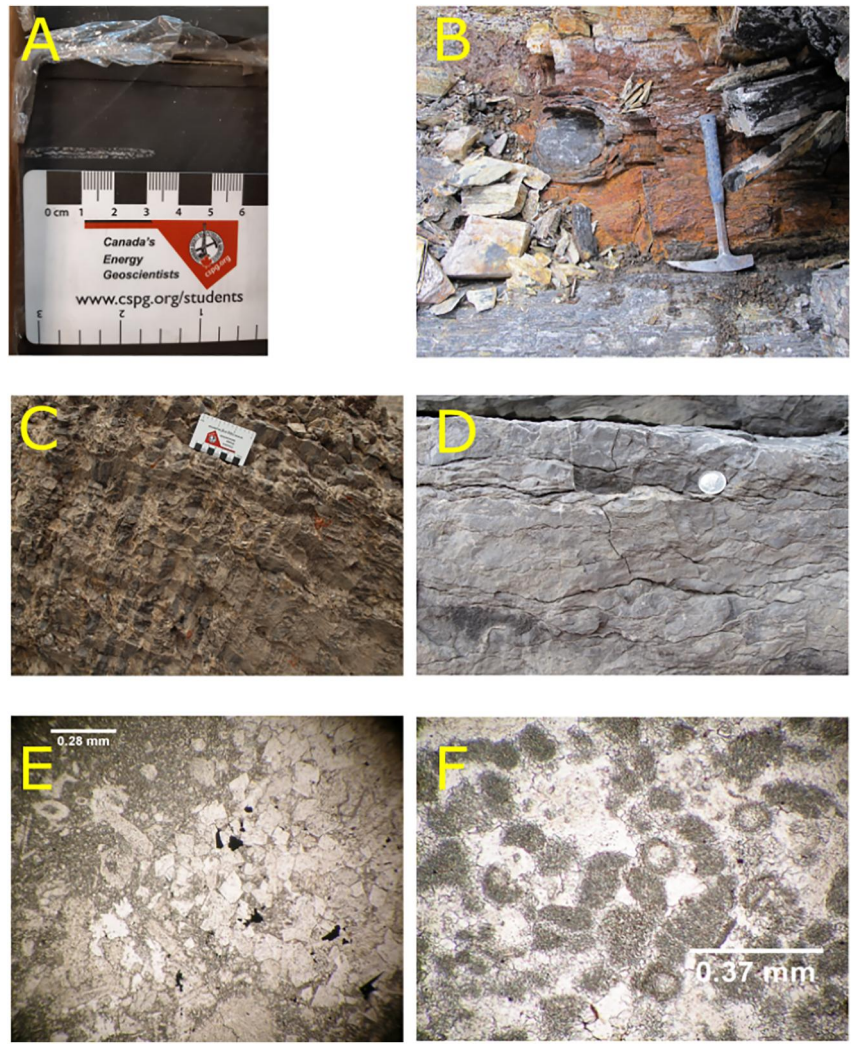

Figure 3. (a) Carbonate concretion observed in the Besa River core. (b) Carbonate concretion observed within the Exshaw Formation at Jura Creek section. (c) Outcrop image of mixed siliciclastic-carbonate sediments of the Sassenach Formation at Snaring, with rock hammer for scale. Thin cyclical deposition of silt and lime mudstone gives the outcrop a striped appearance. (d) Outcrop image of laminated microbialite lithofacies at Crowsnest Pass. Canadian 25-cent coin for scale. (e) Microscope view in plain polarized light (PPL) of euhedral dolomite rhombs within a microspar matrix of carbonate grainstone lithology, Stettler Formation. (f) Microscope view (PPL) of equant blocky isopachous cement surrounding allochems, Stettler Formation. Some of the allochems display broken and recrystallized interiors.

Valley Formation. Finally, this core contains one meter of the Exshaw Formation, which unconformably overlies the Big Valley Formation.

4.2. Values of $\delta^{13}C$ and $\delta^{18}O$

4.2.1. Black Shale Facies (Besa River and Exshaw Formations)

Vertical profiles of $\delta^{13}C$ values show high point-to-point variability (Figures 4 and 5). In the Besa River core, values range from −2.6 to 4.6‰, with a population mean and standard deviation of 0.0 and 1.6‰, respectively (unless otherwise noted, averages and standard deviations reported are population statistics). While sampling was done at an interval of 0.5 m, only 26 of 41 samples had enough $CaCO_3$ for reliable IRMS measurement of carbon and oxygen isotopic ratios. All of these measurements are from fine-grained ground mass and therefore represent disseminated $CaCO_3$ found in the black shale facies; by contrast, a sampled carbonate concretion has a $\delta^{13}C$ value of 3.3‰ from the Besa River core. Another carbonate concretion, from the Exshaw formation at Jura Creek, has a

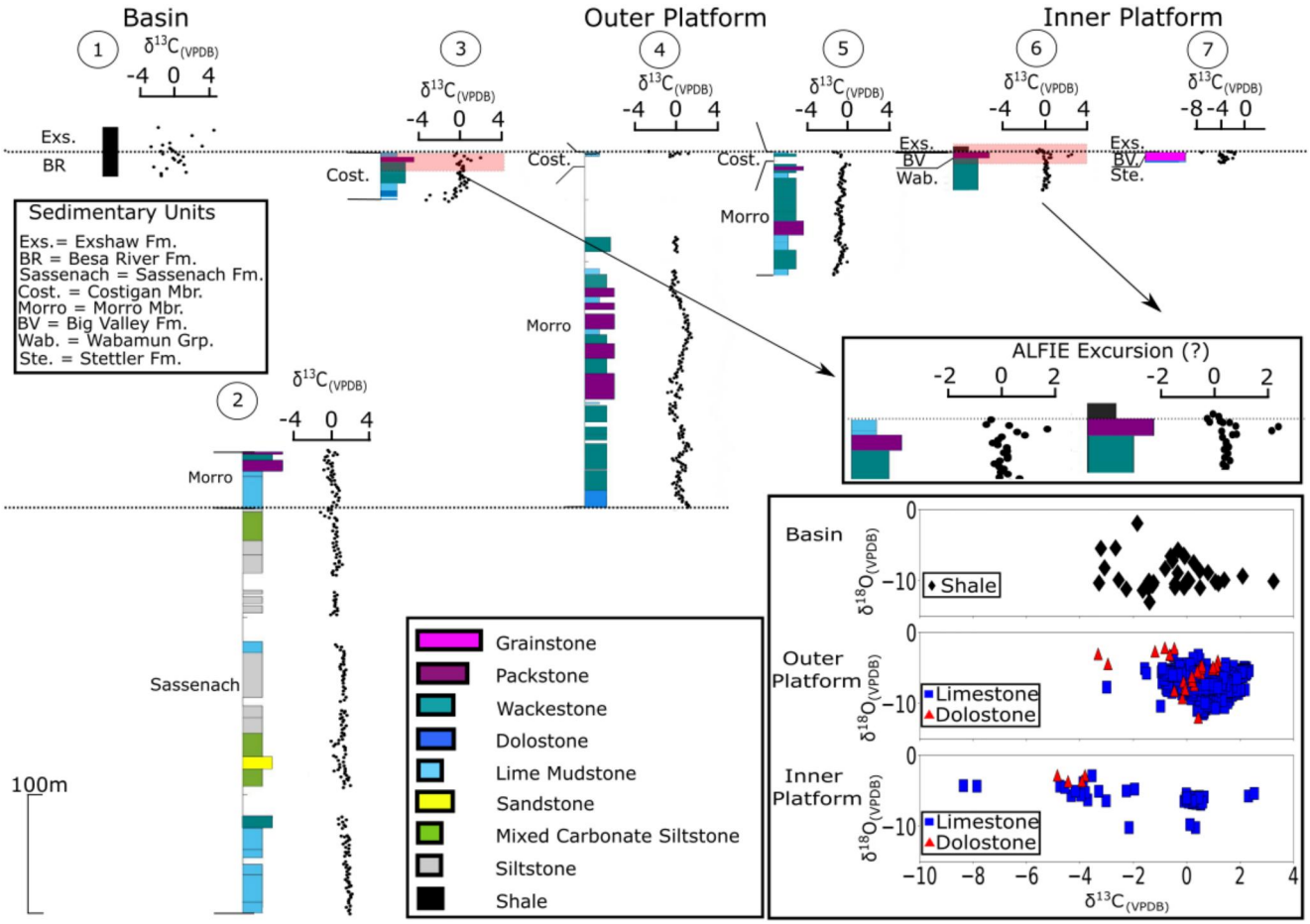

Figure 4. Compilation of studied stratigraphic sections and core sections from the WCSB. 1: Besa River core, 2: Snaring section, 3: Nordegg section, 4: Jura Creek section, 5: Crowsnest Pass section, 6: CNRL Tangent core, 7: Gulf Mohawk core. Costigan and Morro members are abbreviated C. mbr. and M. mbr. respectively. $\delta^{13}C$ versus $\delta^{18}O$ cross-plots show no discernible covariation across all depositional environments. Note the different *x*-axis scales at section 7 relative to sections 1–6.

measured $\delta^{13}C$ value of −3.1‰ (not shown in Figure 4). In the Tangent core, $\delta^{13}C$ values of disseminated $CaCO_3$ in shale range from −0.6 to −0.1‰, with a mean value of −0.3‰ and a standard deviation of 0.2‰ (Figure 4). Here, only 5 of 10 shale samples were measurable via IRMS. In the Gulf Mohawk core, $\delta^{13}C$ values from 3 samples range from −3.2 to −1.9‰, with a mean of −2.6‰ and standard deviation of 0.6‰. Values of $\delta^{18}O$ from carbonates in these shales range from −13.0 to −0.1‰ (Figure 4).

4.2.2. Outer Platform Carbonates (Sassenach and Palliser Formations)

Values of $\delta^{13}C$ measured from carbonates and mixed carbonate-siliciclastic units from the outer platform depositional environment range from −3.3 to 2.3‰ (Figure 5). The mean $\delta^{13}C$ value of the outer platform carbonates is 0.6‰, with a standard deviation of 0.9‰. At Snaring, values of $\delta^{13}C$ show low point-to-point variability in the Sassenach Formation, with a slight negative up-section trend from the base of the Sassenach toward the Palliser contact (Figure 4). At Nordegg, most variability in $\delta^{13}C$ values, as well as the lowest $\delta^{13}C$ values, are observed in the lowermost 7 m, which coincides with dolomite-rich facies (mean $\delta^{13}C$ of this interval is −1.6‰, standard deviation = 1‰; Figure 4). From 8 to 34 m, $\delta^{13}C$ values are relatively constant (mean = 0.1‰, standard deviation = 0.3‰). One outlier is observed at 37 m above the datum, and has a $\delta^{13}C$ value of 1.9‰. At Jura Creek, variability within the section is of similar magnitude as the Snaring section (mean = 0.2‰, standard deviation = 0.6‰). There is a slight positive trend in $\delta^{13}C$ values from 108 to 141 m, reaching a peak value of 1.4‰ (Figure 4). At the contact between the Palliser and Exshaw, there is a prominent outlier of −3.0‰. At Crowsnest Pass, there are no discernible stratigraphic trends (mean = −0.2‰, standard deviation = 0.3‰; Figure 4).

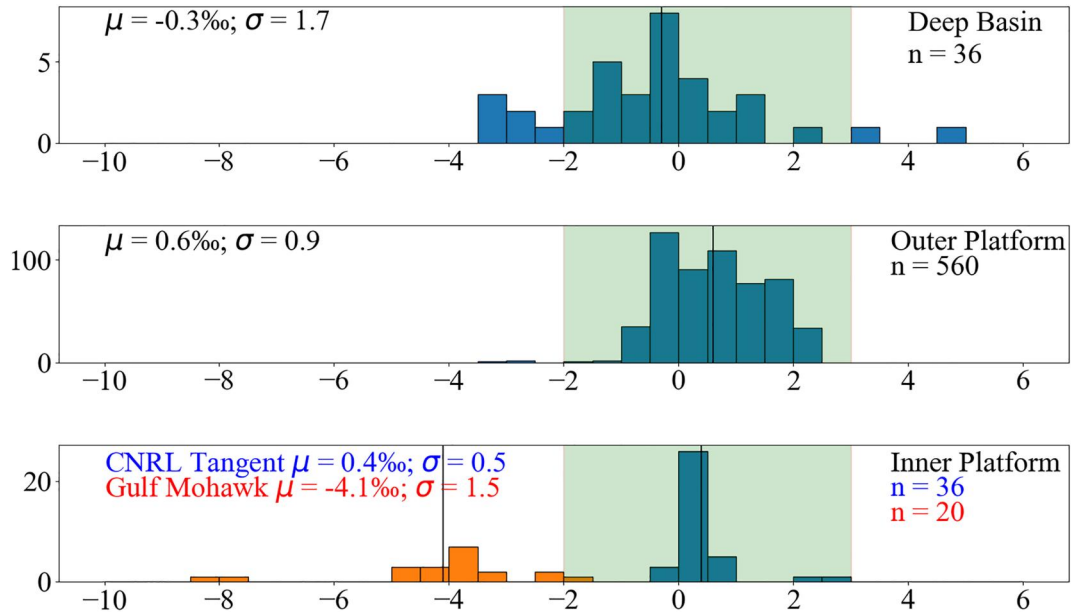

Figure 5. Histogram of $\delta^{13}C$ values of carbonate samples grouped by depositional environments. Population means (μ) and standard deviations (σ) are labeled on the figure; means are plotted as black lines. Green shaded area represents previously published $\delta^{13}C$ values from carbonate from the Devonian Period (Veizer et al., 1999).

Values for $\delta^{18}O$ across the outer platform depositional environment range from −12.0 to −2.1‰ (Figure 4 inset). Overall mean $\delta^{18}O$ is −7.0‰ with a standard deviation of 1.5‰. Generally, variability in $\delta^{18}O$ values are greater than variability in $\delta^{13}C$ values. Dolostone lithofacies have slightly more positive $\delta^{18}O$ values than limestones (dolostone mean = −5.3‰; limestone mean = −7.0‰; Figure 4 inset).

4.2.3. Inner Platform Carbonates (Big Valley, Wabamun and Stettler Formations)

Limestone $\delta^{13}C$ samples in the Tangent core range from −0.1 to 2.5‰, with a mean of 0.4‰ and standard deviation of 0.5‰ (Figures 4 and 5). Values of $\delta^{13}C$ show little stratigraphic variability except for a positive excursion at 1,761.5 m, defined by two data points, with a maximum value of 2.5‰. Dolostone lithologies were not observed within the Tangent core, whereas they dominate the inner platform facies of the Gulf Mohawk core. Here, dolostone $\delta^{13}C$ values range from −4.8 to −3.8‰, with a mean of −4.3‰ and a standard deviation of 0.4‰ (Figures 4 and 5). Limestone $\delta^{13}C$ samples range from −8.4 to −2.0‰, with a mean of −4.1‰ and a standard deviation of 1.7‰. The most negative $\delta^{13}C$ values observed (two measurements, one of −8.4‰ and the other −7.9‰) are observed right below the contact with the Exshaw Formation (Figure 4).

At Tangent, limestone $\delta^{18}O$ values, at Tangent, range from −9.8 to −5.4‰, with a mean of −6.5‰ and a standard deviation of 0.9‰ (Figure 4 inset). At Gulf Mohawk, dolostone $\delta^{18}O$ values range from −3.7 to −2.8‰, with a mean of −3.3‰ and a standard deviation of 0.4‰ (Figure 4 inset). Limestone $\delta^{18}O$ values range from −10.2 to −2.9‰, with a mean of −5.3‰ and a standard deviation of 1.5‰.

4.3. Weight Percent Inorganic Carbon in Shales

Using coulometric titration, the total weight percentage of inorganic carbon (wt % IC) present as disseminated $CaCO_3$ in black shales was measured from 22 out of 54 samples of the Besa River and Exshaw formations, while wt % IC for the remaining 32 were inferred based on IRMS measurements (Figure 6a). High point-to-point variability in wt % IC is observed throughout the shale intervals. Measured values range from 0.01 to 3.15%, with a mean of 0.76% and a standard deviation of 0.78. IRMS-inferred values range from 0.01 to 2.36%, with a mean of 0.40% and a standard deviation of 0.47. In total, 45 of the 54 samples were found to have an inorganic carbon content below 1% and no discernible stratigraphic trends were identified in any of the core sections.

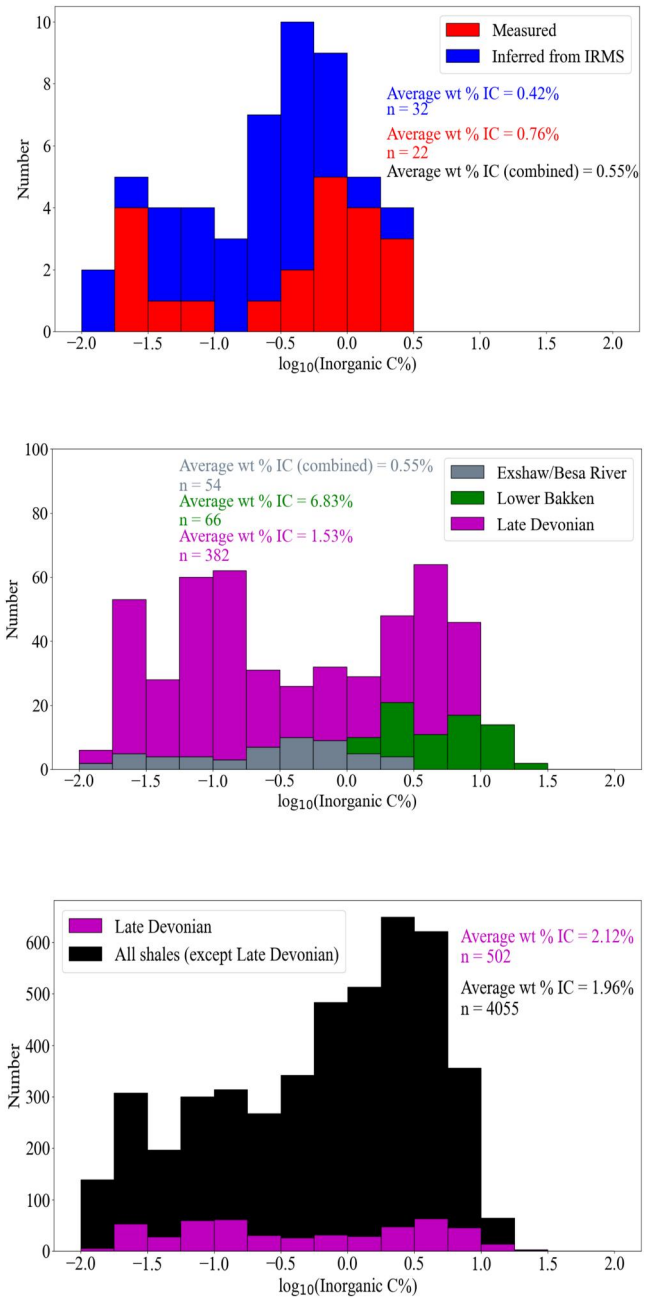

Figure 6. (a) Histogram of inorganic carbon content of shale samples. "Measured" refers to Exshaw and Besa River samples that were directly measured via coulometry, while "Inferred from IRMS" refers to values inferred from the IRMS beam area (Figure S1 in Supporting Information S1) (b) Histogram of inorganic carbon content of samples from this study relative to Late Devonian shales and the Lower Bakken Formation. Exshaw and Besa River values are taken from this study, while Lower Bakken values are from Barnes et al. (2020) and Late Devonian North American shale data are from the USGS National Geochemical Database (USGS, 2008). (c) Histogram of inorganic carbon content of samples from all Late Devonian shales (including the Lower Bakken, Exshaw and Besa River formations, and data from the USGS) compared to shales of other ages from the USGS database.

5. Discussion

The purpose of this study is to evaluate the significance of authigenic carbonate burial for global carbon isotope mass balance, specifically during the Late Devonian. However, the data produced may also be used to discuss regional chemostratigraphy, such as the identification of carbon isotope excursions and interbasinal correlations with excursions identified elsewhere. First, we begin by discussing the validity of the chemostratigraphic trends identified in our results before discussing to what degree the burial flux of authigenic carbonate may have influenced global isotope mass balance.

5.1. Late Famennian Chemostratigraphy

Stratigraphic variation in $\delta^{13}C$ values of marine carbonate may be controlled by early stage meteoric diagenesis, which can overprint primary values of $\delta^{13}C$ (Ripperdan, 2001). The most common evidence for this process is a linear relationship between carbon and oxygen isotopes, which may signal post-depositional water-rock reactions between marine carbonate and meteoric groundwater systems (Allan & Matthews, 1982; Banner & Hanson, 1990). Overall for the entire carbonate $\delta^{13}C$–$\delta^{18}O$ data set, there is no evidence for strong linear correlation ($R^2 = 0.05$). Furthermore, when samples are classified based on depositional environment (basinal, outer platform, inner platform), the strength of correlation between $\delta^{13}C$ and $\delta^{18}O$ values in these data subsets remains low ($R^2 = 0.06$; $R^2 = 0.03$; $R^2 = 0.31$, respectively, Figure 4 inset). However, these approaches can obscure portions of the stratigraphic record in which $\delta^{13}C$ and $\delta^{18}O$ values are well correlated, since samples from different sections and heights are being analyzed together. We address this by calculating R^2 values on individual sections, using a rolling window approach, using a window size of 20 samples. We use this approach to identify portions of stratigraphic sections with a stronger correlation between $\delta^{13}C$ and $\delta^{18}O$ values, defined here as $R^2 > 0.6$. A cutoff $R^2 > 0.6$ is somewhat arbitrary, but allows for a broad range of samples to be identified as being affected by diagenesis. These sample groups occur at Jura Creek (from 10 to 38.5 m and from 42 to 63 m) and at Crowsnest Pass (from 2 to 29 m) (Figure 4; Figure S2 in Supporting Information S1). Thin section analysis of samples within these intervals (Jura Creek at 64 m and Crowsnest Pass at 17 m) revealed extensive interlocking dolomite (at Jura Creek) and scattered burrow-filled dolomite in a recrystallized lime mudstone (at Crowsnest Pass), which potentially supports diagenetic effect on carbon isotopes. A histogram of all R^2 values calculated during this rolling window analysis has a right skew, with values ranging from 0.0 to 0.7 and a median value of 0.1 (Figure S2 in Supporting Information S1).

Overall, there are no significant long - term secular trends in $\delta^{13}C$ value, with a mean value of 0.6‰ across all platform sections combined (the Sassenach, Palliser, Big Valley, and Stettler formations, excluding the Gulf Mohawk core; Figure 4). Furthermore, these $\delta^{13}C$ values do not exceed beyond the accepted range for Devonian seawater (Veizer et al., 1999) (Figure 5). A potential positive excursion, however, does exist in data from the Nordegg and CNRL Tangent sections, at 37 m (max $\delta^{13}C$ value = 1.9‰) and 1,761.5 md (max $\delta^{13}C$ value = 2.5‰) respectively (Figure 4 inset). Both occur within the upper Costigan/Big Valley and thus can be correlated together. Conodonts from within the upper Costigan/Big Valley range from Lower *expansa* to *praesculata* (Johnston et al., 2010).

The presence of positive isotope excursions within these conodont zones may be attributed to the regional Dasberg event, a smaller-scale episode of faunal overturn preceding the more widely known global Hangenberg event (Cole et al., 2015; Hartenfels & Becker, 2009; Myrow et al., 2011). A carbon isotope excursion has been proposed to co-occur with this event referred to as the Late Famennian Isotope Excursion (ALFIE) based on data from stratigraphic sections in the western United States (Myrow et al., 2011). This excursion has been interpreted as representing enhanced carbon burial linked to a warmer period, interrupting the overall global cooling trend that characterized the Late Devonian—Early Carboniferous (Myrow et al., 2011; Sandberg et al., 2002). Sedimentologically, the Dasberg event is characterized by a marine regression, followed by the development of an unconformity and subsequent transgressive deposition of black shales, consistent with field observations in sections found in the WCSB (Hartenfels & Becker, 2009; Sandberg et al., 2002).

5.2. The $\delta^{13}C$ Value of Late Devonian Shale-Hosted Carbonates

In order for authigenic carbonate to have an effect on global carbon isotope mass balance, it needs to be both voluminous and have negative $\delta^{13}C$ values (i.e., display a significant isotopic offset from coeval marine carbonates). The Famennian represents an ideal time period to assess this hypothesis owing to the sedimentological conditions that might foster the precipitation of authigenic carbonate: a sharp areal restriction in shelfal carbonate depositional systems (Barnes et al., 2020; Kaiser et al., 2016; Peterhänsel et al., 2008; van Loevezijn & Raven, 2017) and expanded ocean anoxia (Becker et al., 2016; Kaiser et al., 2006; Marynowski et al., 2012; Schieber & Baird, 2001).

As opposed to marine carbonates, carbonate minerals within basinal shales are hypothesized to have precipitated under anoxic conditions during organic carbon respiration and thus be more negative on average than the carbonate sink (Coleman & Raiswell, 1993; Higgins et al., 2009; Mitnick et al., 2018; Mozley & Burns, 1993; Schrag et al., 2013). The observed range of $\delta^{13}C$ values of disseminated carbonate (including concretions) in shales is large (−3.2–4.6‰). The variability of $\delta^{13}C$ values in shale carbonates is also pronounced within the two carbonate concretions sampled, both from the lower Exshaw Formation at Jura Creek and within the Besa River core section (−3.1 and 3.3‰, respectively). This spread in values may reflect the variability of local diagenetic processes. For example, the precipitation within localized zones of methanogenesis should lead to more positive values (Claypool & Kaplan, 1974), while precipitation in the presence of organic matter degradation should lead to more negative values. When considered together, these processes yield average $\delta^{13}C$ values from carbonate within the Besa River and the Exshaw formations that approximate marine carbonate values.

One possible explanation for the rather muted $\delta^{13}C$ variability in these shale carbonates is a larger Late Devonian DIC reservoir (e.g., 10–15 times greater than present day; (Berner, 2006)). Higher levels of Devonian DIC could result in a higher diffusive flux of seawater DIC into marine sediments, meaning that it would be more difficult for $\delta^{13}C$ of porewater DIC to diverge significantly from seawater. Regardless of the exact mechanism that explains the $\delta^{13}C$ values in these shale-hosted carbonates, as long as the carbonate cements are formed early enough as to remain in diffusive contact with the overlying water-column, their importance to global carbon isotope mass balance will be dictated by their mass burial flux and their average $\delta^{13}C$ value. The difference in average $\delta^{13}C$ between shale carbonates and outer platform carbonates in this study is very slight (−0.3 vs. 0.6‰, respectively; Figure 5).

For these mean calculations, samples from stratigraphic intervals with $\delta^{13}C$–$\delta^{18}O$ R^2 values greater than 0.6 have been excluded. These excluded samples (Jura Creek: from 10 to 38.5 m and from 42 to 63 m, and Crowsnest Pass: from 2 to 29 m) correspond to recrystallized dolomitic lime mudstone within the Morro Member of the greater Palliser Formation. If we consider all data points, the difference in average $\delta^{13}C$ between shale carbonates and outer platform carbonates remains unchanged (−0.3 vs. 0.6‰, respectively). Despite concerns about diagenesis revealed by the rolling window analysis, calculations of average $\delta^{13}C$ values between the different depositional settings remain fairly robust. The lack of appreciably different $\delta^{13}C$ values between basinal carbonate and platformal carbonates suggests that enhanced burial of authigenic carbonate will not have a significant enrichment effect on the $\delta^{13}C$ value of DIC. Similar findings have been reported from other studies on authigenic carbonate-hosted formation across the Paleozoic (Barnes et al., 2020; Gaines & Vorhies, 2016; Saitoh et al., 2015).

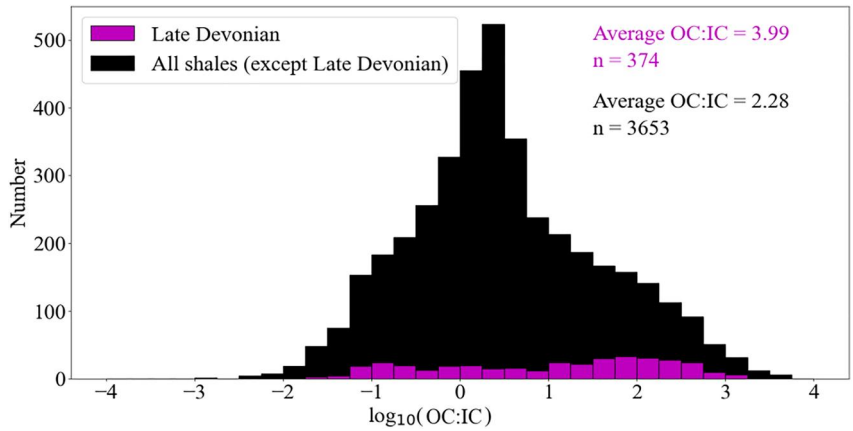

Figure 7. Histogram of organic carbon (OC) to inorganic carbon (IC) mass ratios on shale units from the USGS database. Average values are calculated as the mean weight percent OC divided by the mean weight percent IC for each category. The histogram is divided into samples that are either exclusively Late Devonian-aged (pink) or Phanerozoic in age, omitting the Late Devonian (black). Note that certain samples did not have data for both organic carbon wt % and inorganic carbon wt %, thus resulting in sample counts which are lower than Figure 6c.

5.3. The Effect of Authigenic Carbonate Burial on the Late Devonian Carbon Cycle

In addition to a required large isotopic offset between marine carbonate and authigenic carbonate, the burial flux of authigenic carbonate must be comparable to mass burial fluxes of marine carbonate and organic carbon in order for authigenic carbonate to be important for isotope mass balance. To test this assumption, weight percent inorganic carbon was measured from the black shales of the Besa River and Exshaw formations. While we make the assumption that all inorganic carbon within shale samples are authigenic in origin, the origin of this carbonate is not important to constrain the flux of carbonate in silcicilastic units, so long as the carbonate is primary or formed during early diagenesis. Furthermore, we assume that most of the carbonate is formed as fine-grained disseminations. The presence of macroscopic carbonate concretions, dependant on size and abundance, may result in a larger mass burial flux of authigenic carbonate. Therefore, the following calculations represent a lower bound estimate of the Late Devonian authigenic carbonate sink. Weight percent inorganic carbon (wt % IC) values are highly variable, ranging from negligible amounts to as high as 3.15% (occurring in the CNRL Tangent core). Mean wt % IC (both directly measured via coulometry and inferred from IRMS peak sizes) for all sections is 0.55% (the average for coulometry-measured is 0.76% and for IRMS-inferred is 0.42%; Figure 6a). These values, however, are low when compared to the Lower Bakken Formation, which overlaps in age with the Exshaw and was deposited in an adjacent intracratonic sedimentary basin (Barnes et al., 2020) and shows much higher wt % IC values (average = 6.8%; Figure 6b). This comparison suggests that intracratonic basins could host a higher burial flux of authigenic carbonate relative to more open marine depositional settings. Reasons for this observation warrant further investigation.

It must be noted that results from the WCSB may be prone to sampling bias owing to the relatively few samples measured. In order to expand the amount of data analyzed to explore whether a significant amount of $CaCO_3$ was buried in shales during the Late Devonian, we used the USGS National Geochemical database. Inorganic carbon content of Late Devonian shales in this database is compared to North American shales across the Late Precambrian and Phanerozoic. Late Devonian shales (N = 502) have only slightly higher amounts of carbonate (average = 2.12%, 2 standard errors on the mean (2 S.E.) = 0.29) relative to other shales (average wt % IC = 1.96%, 2 S.E. = 0.08, N = 4,055; Figure 6c). However, these mean values overlap at the 2 S.E. level, meaning that the difference in values is not likely significant. These results from North American shales do not support the notion of an expanded authigenic carbonate sink during the Late Devonian.

The mass ratio of organic carbon to inorganic carbon in shales is also instructive in assessing the role of fine-grained siliciclastics in the global carbon cycle. If the inorganic carbon content of marine shales is higher than organic carbon (i.e. OC:IC < 1), this would imply that the burial flux of carbonate in these units would be higher than that of organic carbon. Shales from the USGS database have OC:IC mass ratios that are generally greater than 1, both for shales of various ages and Late Devonian shales (Figure 7). Average ratios, calculated as average

wt % (OC)/average wt % (IC), are 3.99 for Late Devonian shales and 2.28 for all other aged units. The implication of these OC:IC ratios is that an increase in shale deposition most notably increases the burial flux of organic carbon, rather than carbonate carbon. This is also true in the Late Devonian, which even if they display very slightly elevated values in weight percent inorganic carbon (2.12% vs. 1.96%), Late Devonian units also have a higher OC:IC ratio compared to the Phanerozoic average (3.99 vs. 2.28).

5.4. A Low $\delta^{13}C$ Carbon Sink Within Restricted Inner Carbonate Platforms

Despite the lack of long-term trends in $\delta^{13}C$ values in outer and inner platform carbonates, local signals amongst the stratigraphic sections are observable. Negative values found in the Nordegg section are associated with dolostone lithologies and are likely attributable to diagenesis (Figure 4). The Gulf Mohawk core is distinct from the other stratigraphic sections as it features negative $\delta^{13}C$ values throughout (mean value = −4.1‰, with the most negative value (−8.4‰) found right below the Exshaw contact; Figures 4 and 5), much lower on average than disseminated $CaCO_3$ found in shales. A possible explanation for these low $\delta^{13}C$ values is the respiration of organic matter in the local water column of the inner platform. In this scenario, both terrestrial and marine organic matter would have accumulated in the proximal platform environment and combined with the increased residence time and poor mixing of inner shelf waters with the open ocean, could have resulted in low $\delta^{13}C$ values in the water column (and any carbonates that precipitate from these waters). This explanation has been previously applied to modern low $\delta^{13}C$ values in DIC found in Florida Bay, which is a depositional environment that is analogous to Famennian carbonates of the WCSB (Lloyd, 1964; Patterson & Walter, 1994).

Alternatively, carbonates in Gulf Mohawk could have been reset to more negative $\delta^{13}C$ values during early meteoric diagenesis, as a result of organic carbon respiration in soil profiles (Allan & Matthews, 1982), as these sediments show evidence for recrystallization and dolomitization (Figures 3c and 3d). However, this interpretation is doubtful as there is no covariation between $\delta^{13}C$ and $\delta^{18}O$ data (Figure S2 in Supporting Information S1), which is common in meteorically altered carbonates. Regardless of the exact mechanism, the burial of these shallow-water carbonates with low $\delta^{13}C$ values would have a similar effect as the proposed authigenic carbonate sink on the carbon isotope composition of DIC, provided that these types of altered carbonates are abundant. It is conceivable that periods in Earth History, such as times of eustatic sea-level fall, could have expanded the area and occurrence of these restricted shallow marine environments, and previous modeling efforts show that the increased meteoric diagenesis, during sea-level lowstands, could encourage a significant sink of ^{13}C-depleted carbon (Dyer et al., 2015).

6. Conclusions

It has been proposed that the burial of authigenic carbonate within fine-grained marine siliciclastic formations represents an overlooked sink for carbon, whereby sedimentary diagenesis in conjunction with anaerobic degradation of organic matter may form carbonate minerals with low $\delta^{13}C$ values. Increased burial of this authigenic carbonate would therefore result in an overall increase in seawater DIC $\delta^{13}C$ values recorded as positive excursions in marine carbonates. Sedimentological and geochemical data predict paleoenvironmental conditions that could be favorable to the presence of an authigenic sink during the Famennian Age (372.2–358.9 Ma.). However, similar average values of carbonate $\delta^{13}C$ values from basinal shales (mean = −0.3‰) and outer platform carbonates (mean = 0.6‰) suggests that carbonates buried in shales could not have had a significant effect on Devonian carbon isotope mass balance. Furthermore, the mass abundance of authigenic carbonate does not appear to be significantly elevated during the Late Devonian (average weight percent inorganic carbon = 2.12%) versus average Phanerozoic shale (1.95%). Lastly, ratios of organic carbon to inorganic carbon show that fine-grained marine siliciclastic units predominantly bury organic carbon rather than carbonate minerals (Late Devonian Shales: OC:IC = 3.99; non-Late Devonian shales: OC:IC = 2.28; Figure 7). All together, these data suggest that the burial flux of inorganic carbon stored as authigenic carbonate did not play a significant role in influencing the $\delta^{13}C$ value of DIC in the Late Devonian.

Data Availability Statement

The data set for this research can be found in the Zenodo data repository and can be accessed via https://doi.org/10.5281/zenodo.10247187 (Gazdewich et al., 2023, December).

Acknowledgments
The authors wish to acknowledge the following for their contribution to this paper. Drill core samples were made available courtesy of the Alberta Energy Regulator Core Research Centre and the British Columbia Energy Regulator Core Research Facility. Parks Canada for allowing access and permission to sample within Jasper National Park. Laboratory work at the University of Victoria was assisted by Connor van Wieren and Erinn Raferty. Prior to submission, this manuscript was improved with valuable feedback from Benjamin Barnes. The authors wish to also thank reviewers Cedric Hagen and three anonymous reviewers for their feedback. Lastly, this research was funded by a Natural Sciences and Engineering Research Council of Canada (NSERC) Discovery Grant to J. Husson (RGPIN-2017-03887).

References

Allan, J., & Matthews, R. (1982). Isotope signatures associated with early meteoric diagenesis. *Sedimentology*, *29*(6), 797–817. https://doi.org/10.1111/j.1365-3091.1982.tb00085.x

Banner, J. L., & Hanson, G. N. (1990). Calculation of simultaneous isotopic and trace element variations during water-rock interaction with applications to carbonate diagenesis. *Geochimica et Cosmochimica Acta*, *54*(11), 3123–3137. https://doi.org/10.1016/0016-7037(90)90128-8

Barnes, B. D., Husson, J. M., & Peters, S. E. (2020). Authigenic carbonate burial in the Late Devonian–Early Mississippian Bakken Formation (Williston Basin, USA). *Sedimentology*, *67*(4), 2065–2094. https://doi.org/10.1111/sed.12695

Becker, R. T., Kaiser, S. I., & Aretz, M. (2016). Review of chrono-litho-and biostratigraphy across the global Hangenberg Crisis and Devonian–Carboniferous Boundary. *Geological Society, London, Special Publications*, *423*(1), 355–386. https://doi.org/10.1144/sp423.10

Berner, R. A. (2006). GEOCARBSULF: A combined model for Phanerozoic atmospheric O_2 and CO_2. *Geochimica et Cosmochimica Acta*, *70*(23), 5653–5664. https://doi.org/10.1016/j.gca.2005.11.032

Berner, R. A., & Kothavala, Z. (2001). GEOCARB III: A revised model of atmospheric CO_2 over Phanerozoic time. *American Journal of Science*, *301*(2), 182–204. https://doi.org/10.2475/ajs.301.2.182

Bradbury, H. J., & Turchyn, A. V. (2019). Reevaluating the carbon sink due to sedimentary carbonate formation in modern marine sediments. *Earth and Planetary Science Letters*, *519*, 40–49. https://doi.org/10.1016/j.epsl.2019.04.044

Catling, D. C., & Claire, M. W. (2005). How Earth's atmosphere evolved to an oxic state: A status report. *Earth and Planetary Science Letters*, *237*(1–2), 1–20. https://doi.org/10.1016/j.epsl.2005.06.013

Claypool, G. E., & Kaplan, I. R. (1974). The origin and distribution of methane in marine sediments. In I. R. Kaplan (Ed.), *Natural gases in marine sediments. Marine science* (Vol. 3). Springer. https://doi.org/10.1007/978-1-4684-2757-8_8

Cole, D., Myrow, P., Fike, D., Hakim, A., & Gehrels, G. E. (2015). Uppermost Devonian (Famennian) to Lower Mississippian events of the western US: Stratigraphy, sedimentology, chemostratigraphy, and detrital zircon geochronology. *Palaeogeography, Palaeoclimatology, Palaeoecology*, *427*, 1–19. https://doi.org/10.1016/j.palaeo.2015.03.014

Coleman, M., & Raiswell, R. (1993). Microbial mineralization of organic matter: Mechanisms of self-organization and inferred rates of precipitation of diagenetic minerals. *Philosophical Transactions of the Royal Society of London. Series A: Physical and Engineering Sciences*, *344*(1670), 69–87.

Cramer, B. D., Saltzman, M. R., Day, J. E., & Witzke, B. J. (2008). Record of the Late Devonian Hangenberg global positive carbon-isotope excursion in an epeiric sea setting: Carbonate production, organic-carbon burial and paleoceanography during the Late Famennian. In H. Holmden & B. R. Pratt (Eds.), *Dynamics of Epeiric seas: Sedimentological, paleontological and geochemical perspectives* (Vol. 48, pp. 103–118). Geological Association of Canada, Special Paper.

Derry, L. A. (2015). Causes and consequences of mid-Proterozoic anoxia. *Geophysical Research Letters*, *42*(20), 8538–8546. https://doi.org/10.1002/2015gl065333

de Witt, R., & McLaren, D. (1950). Devonian sections in the Rocky Mountain's between Crowsnest Pass and Jasper, Alberta. Geological Survey of Canada Paper 50-23 (p. 409).

Dunham, R. J. (1962). Classification of carbonate rocks according to depositional textures. In *Classification of carbonate rocks* (pp. 108–121). AAPG Special Volumes.

Dyer, B., Maloof, A. C., & Higgins, J. A. (2015). Glacioeustasy, meteoric diagenesis, and the carbon cycle during the Middle Carboniferous. *Geochemistry, Geophysics, Geosystems*, *16*(10), 3383–3399. https://doi.org/10.1002/2015gc006002

Fantle, M. S., Barnes, B. D., & Lau, K. V. (2020). The role of diagenesis in shaping the geochemistry of the marine carbonate record. *Annual Review of Earth and Planetary Sciences*, *48*(1), 549–583. https://doi.org/10.1146/annurev-earth-073019-060021

Ferri, F., Hickin, A. S., & Huntley, D. H. (2011). Besa River Formation, western Liard Basin, British Columbia (NTS 094N): Geochemistry and regional correlations. In *British Columbia Ministry of Energy and Mines Geoscience Reports*, 1–18.

Ferri, F., McMechan, M., Richards, B., & Friedman, R. (2021). Organic-rich upper Devonian shales of the Patry and Exshaw Formations (Besa River group) in the subsurface of Liard Basin. In *British Columbia Ministry of Energy, Mines and Low Carbon Innovation, British Columbia Geological Survey Paper 2021-01*, (p. 42).

Gaines, R. R., & Vorhies, J. S. (2016). Growth mechanisms and geochemistry of carbonate concretions from the Cambrian Wheeler Formation (Utah, USA). *Sedimentology*, *63*(3), 662–698. https://doi.org/10.1111/sed.12234

Gazdewich, S., Husson, J., & Hauck, T. (2023). Authigenic carbonate burial within the Late Devonian Western Canada Sedimentary Basin and its impact on the global carbon cycle [Dataset]. https://doi.org/10.5281/zenodo.10247187

Geyman, E. C., & Maloof, A. C. (2019). A diurnal carbon engine explains ^{13}C-enriched carbonates without increasing the global production of oxygen. *Proceedings of the National Academy of Sciences of the United States of America*, *116*(49), 24433–24439. https://doi.org/10.1073/pnas.1908783116

Grotzinger, J. P., Fike, D. A., & Fischer, W. W. (2011). Enigmatic origin of the largest-known carbon isotope excursion in Earth's history. *Nature Geoscience*, *4*(5), 285–292. https://doi.org/10.1038/ngeo1138

Grotzinger, J. P., & Knoll, A. H. (1995). Anomalous carbonate precipitates: Is the Precambrian the key to the Permian? *Palaios*, *10*(6), 578–596. https://doi.org/10.2307/3515096

Halbertsma, H. L. (1994). Devonian Wabamun group of the western Canada sedimentary basin. In G. Mossop, & I. Shetsen (Eds.), *Geological Atlas of the western Canada sedimentary basin* (pp. 203–220). Canadian Society of Petroleum Geologists and Alberta Research Council

Halverson, G. P., Hoffman, P. F., Schrag, D. P., Maloof, A. C., & Rice, A. H. N. (2005). Toward a Neoproterozoic composite carbon-isotope record. *GSA Bulletin*, *117*(9–10), 1181–1207. https://doi.org/10.1130/b25630.1

Hartenfels, S., & Becker, R. T. (2009). Timing of the global Dasberg Crisis–implications for Famennian eustasy and chronostratigraphy. *Palaeontographica Americana*, *63*, 71–97.

Hay, C. C., Creveling, J. R., Hagen, C. J., Maloof, A. C., & Huybers, P. (2019). A library of early Cambrian chemostratigraphic correlations from a reproducible algorithm. *Geology*, *47*(5), 457–460. https://doi.org/10.1130/g46019.1

Higgins, J. A., Fischer, W., & Schrag, D. (2009). Oxygenation of the ocean and sediments: Consequences for the seafloor carbonate factory. *Earth and Planetary Science Letters*, *284*(1–2), 25–33. https://doi.org/10.1016/j.epsl.2009.03.039

Johnston, D. I., Henderson, C. M., & Schmidt, M. J. (2010). Upper Devonian to Lower Mississippian conodont biostratigraphy of uppermost Wabamun Group and Palliser Formation to lowermost Banff and Lodgepole formations, southern Alberta and southeastern British Columbia, Canada: Implications for correlations and sequence stratigraphy. *Bulletin of Canadian Petroleum Geology*, *58*(4), 295–341. https://doi.org/10.2113/gscpgbull.58.4.295

Johnston, D. T., Macdonald, F. A., Gill, B., Hoffman, P., & Schrag, D. P. (2012). Uncovering the Neoproterozoic carbon cycle. *Nature*, *483*(7389), 320–323. https://doi.org/10.1038/nature10854

Jones, D. S., Brothers, R. W., Crüger Ahm, A.-S., Slater, N., Higgins, J. A., & Fike, D. A. (2020). Sea level, carbonate mineralogy, and early diagenesis controlled $\delta^{13}C$ records in Upper Ordovician carbonates. *Geology*, *48*(2), 194–199. https://doi.org/10.1130/g46861.1

Kaiser, S. I., Aretz, M., & Becker, R. T. (2016). The global Hangenberg Crisis (Devonian–Carboniferous transition): Review of a first-order mass extinction. *Geological Society, London, Special Publications*, *423*(1), 387–437. https://doi.org/10.1144/sp423.9

Kaiser, S. I., Steuber, T., Becker, R. T., & Joachimski, M. M. (2006). Geochemical evidence for major environmental change at the Devonian–Carboniferous boundary in the Carnic Alps and the Rhenish Massif. *Palaeogeography, Palaeoclimatology, Palaeoecology*, *240*(1–2), 146–160. https://doi.org/10.1016/j.palaeo.2006.03.048

Kaylor, D. (1988). Facies and diagenesis of the Upper Devonian Palliser Formation, Front Ranges of the southern Rocky Mountains, Alberta and BC unpublished M. Sc. [Master's thesis, thesis]. McGill University.

Knoll, A., Hayes, J., Kaufman, A., Swett, K., & Lambert, I. (1986). Secular variation in carbon isotope ratios from Upper Proterozoic successions of Svalbard and East Greenland. *Nature*, *321*(6073), 832–838. https://doi.org/10.1038/321832a0

Kump, L., & Arthur, M. A. (1999). Interpreting carbon-isotope excursions: Carbonates and organic matter. *Chemical Geology*, *161*(1–3), 181–198. https://doi.org/10.1016/s0009-2541(99)00086-8

Kump, L., & Garrels, R. M. (1986). Modeling atmospheric O_2 in the global sedimentary redox cycle. *American Journal of Science*, *286*(5), 337–360. https://doi.org/10.2475/ajs.286.5.337

Lloyd, R. M. (1964). Variations in the oxygen and carbon isotope ratios of Florida Bay mollusks and their environmental significance. *The Journal of Geology*, *72*(1), 84–111. https://doi.org/10.1086/626966

Macqueen, R. W., & Sandberg, C. A. (1970). Stratigraphy, age, and interregional correlation of the Exshaw Formation, Alberta Rocky Mountains. *Bulletin of Canadian Petroleum Geology*, *18*(1), 32–66.

Marynowski, L., Zatoń, M., Rakociński, M., Filipiak, P., Kurkiewicz, S., & Pearce, T. J. (2012). Deciphering the upper Famennian Hangenberg Black Shale depositional environments based on multi-proxy record. *Palaeogeography, Palaeoclimatology, Palaeoecology*, *346*, 66–86. https://doi.org/10.1016/j.palaeo.2012.05.020

McLaren, D. J., & Mountjoy, E. W. (1962). *Alexo equivalents in the Jasper region*. Department of Mines; Technical Surveys.

Meijer-Drees, N. C., Richards, B. C., & Johnston, D. (1993). The Devonian Palliser Formation and its equivalents, southern Alberta, Canada. *Geological Survey of Canada, Open File*, *2698*, 69. https://doi.org/10.4095/193347

Milliman, J. D. (1993). Production and accumulation of calcium carbonate in the ocean: Budget of a nonsteady state. *Global Biogeochemical Cycles*, *7*(4), 927–957. https://doi.org/10.1029/93gb02524

Mitnick, E. H., Lammers, L. N., Zhang, S., Zaretskiy, Y., & DePaolo, D. J. (2018). Authigenic carbonate formation rates in marine sediments and implications for the marine $\delta^{13}C$ record. *Earth and Planetary Science Letters*, *495*, 135–145. https://doi.org/10.1016/j.epsl.2018.05.018

Mountjoy, E. (1980). Some questions about the development of Upper Devonian carbonate buildups (reefs), Western Canada. *Bulletin of Canadian Petroleum Geology*, *28*(3), 315–344.

Mozley, P. S., & Burns, S. J. (1993). Oxygen and carbon isotopic composition of marine carbonate concretions; an overview. *Journal of Sedimentary Research*, *63*(1), 73–83. https://doi.org/10.1306/d4267a91-2b26-11d7-8648000102c1865d

Müller, R. D., Roest, W. R., Royer, J.-Y., Gahagan, L. M., & Sclater, J. G. (1997). Digital isochrons of the world's ocean floor. *Journal of Geophysical Research*, *102*(B2), 3211–3214. https://doi.org/10.1029/96jb01781

Myrow, P. M., Strauss, J. V., Creveling, J. R., Sicard, K. R., Ripperdan, R., Sandberg, C. A., & Hartenfels, S. (2011). A carbon isotopic and sedimentological record of the latest Devonian (Famennian) from the Western US and Germany. *Palaeogeography, Palaeoclimatology, Palaeoecology*, *306*(3–4), 147–159. https://doi.org/10.1016/j.palaeo.2011.04.013

Oehlert, A. M., & Swart, P. K. (2014). Interpreting carbonate and organic carbon isotope covariance in the sedimentary record. *Nature Communications*, *5*(1), 1–7. https://doi.org/10.1038/ncomms5672

Patterson, W. P., & Walter, L. M. (1994). Depletion of ^{13}C in seawater ΣCO_2 on modern carbonate platforms: Significance for the carbon isotopic record of carbonates. *Geology*, *22*(10), 885–888. https://doi.org/10.1130/0091-7613(1994)022<0885:docisc>2.3.co;2

Peterhänsel, A., Pratt, B. R., & Holmden, C. (2008). The Famennian (Upper Devonian) Palliser platform of Western Canada–architecture and depositional dynamics of a post-extinction epeiric giant. In *Dynamics of Epeiric Seas: Geological Society of Canada Special Paper* (Vol. 48, pp. 247–281).

Peters, S. E., Husson, J. M., & Czaplewski, J. (2018). Macrostrat: A platform for geological data integration and deep-time Earth crust research. *Geochemistry, Geophysics, Geosystems*, *19*(4), 1393–1409. https://doi.org/10.1029/2018gc007467

Planavsky, N. J., Reinhard, C. T., Wang, X., Thomson, D., McGoldrick, P., Rainbird, R. H., et al. (2014). Low Mid-Proterozoic atmospheric oxygen levels and the delayed rise of animals. *Science*, *346*(6209), 635–638. https://doi.org/10.1126/science.1258410

Richards, B., Bamber, E., Henderson, C., Higgins, A., Johnston, D., Mamet, B., & Meijer-Drees, N. (1993). Uppermost Devonian (Famennian) and Lower Carboniferous (Tournaisian) at Jura Creek, and Mount Rundle, southwestern Alberta. *Geological Survey of Canada*. Open File, 2866, 81. https://doi.org/10.4905/194058

Richards, B., & Higgins, A. (1988). Devonian-Carboniferous boundary beds of the Palliser and Exshaw formations at Jura Creek, Rocky Mountains, southwestern Alberta.

Ripperdan, R. L. (2001). Stratigraphic variation in marine carbonate carbon isotope ratios. *Reviews in Mineralogy and Geochemistry*, *43*(1), 637–662. https://doi.org/10.2138/gsrmg.43.1.637

Riquier, L., Tribovillard, N., Averbuch, O., Devleeschouwer, X., & Riboulleau, A. (2006). The Late Frasnian Kellwasser horizons of the Harz Mountains (Germany): Two oxygen-deficient periods resulting from different mechanisms. *Chemical Geology*, *233*(1–2), 137–155. https://doi.org/10.1016/j.chemgeo.2006.02.021

Saitoh, M., Ueno, Y., Isozaki, Y., Shibuya, T., Yao, J., Ji, Z., et al. (2015). Authigenic carbonate precipitation at the end-Guadalupian (Middle Permian) in China: Implications for the carbon cycle in ancient anoxic oceans. *Progress in Earth and Planetary Science*, *2*(1), 41. https://doi.org/10.1186/s40645-015-0073-2

Sandberg, C. A., Morrow, J. R., & Ziegler, W. (2002). *Late Devonian sea-level changes, catastrophic events, and mass extinctions* (pp. 473–488). Special Papers-Geological Society of America.

Savoy, L. E., Harris, A. G., & Mountjoy, E. W. (1999). Extension of lithofacies and conodont biofacies models of Late Devonian to Early Carboniferous carbonate ramp and black shale systems, southern Canadian Rocky Mountains. *Canadian Journal of Earth Sciences*, *36*(8), 1281–1298. https://doi.org/10.1139/cjes-36-8-1281

Schieber, J., & Baird, G. (2001). On the origin and significance of pyrite spheres in Devonian black shales of North America. *Journal of Sedimentary Research*, *71*(1), 155–166. https://doi.org/10.1306/051600710155

Schrag, D. P., Higgins, J. A., Macdonald, F. A., & Johnston, D. T. (2013). Authigenic carbonate and the history of the global carbon cycle. *Science*, *339*(6119), 540–543. https://doi.org/10.1126/science.1229578

Scott, C., Slack, J. F., & Kelley, K. D. (2017). The hyper-enrichment of V and Zn in black shales of the Late Devonian-Early Mississippian Bakken Formation (USA). *Chemical Geology*, *452*, 24–33. https://doi.org/10.1016/j.chemgeo.2017.01.026

Smith, M. G., & Bustin, R. M. (2000). Late Devonian and Early Mississippian Bakken and Exshaw black shale source rocks, Western Canada Sedimentary Basin: A sequence stratigraphic interpretation. *AAPG Bulletin*, *84*(7), 940–960. https://doi.org/10.1306/a9673b76-1738-11d7-8645000102c1865d

Sun, X., & Turchyn, A. V. (2014). Significant contribution of authigenic carbonate to marine carbon burial. *Nature Geoscience*, *7*(3), 201–204. https://doi.org/10.1038/ngeo2070

USGS. (2008). *Geochemistry of rock samples from the national geochemical database (U.S. Geological Survey Open-File Report)* (Vol. 97). US Geological Survey.

van Loevezijn, G. B., & Raven, J. (2017). From carbonate platform to Euxinic Sea–the collapse of an Early/Middle Devonian reef, Cantabrian Mountains (Spain). *Geologos*, *23*(3), 143–161. https://doi.org/10.1515/logos-2017-0018

Veizer, J., Ala, D., Azmy, K., Bruckschen, P., Buhl, D., Bruhn, F., et al. (1999). $^{87}Sr/^{86}Sr$, $\delta^{13}C$ and $\delta^{18}O$ evolution of Phanerozoic seawater. *Chemical Geology*, *161*(1–3), 59–88. https://doi.org/10.1016/s0009-2541(99)00081-9

Workum, R. H., & Hedinger, A. S. (1992). Devonian Frasnian stratigraphy, Rocky Mountain Front Ranges Crowsnest Pass to Jasper, Alberta. *Geological Survey of Canada, Open File*, 2509. https://doi.org/10.4095/133375

Erratum

The originally published version of this article contained a typographical error. In the seventh sentence of the Abstract, beginning "Results show that basinal shale . . .," "(0.4‰)" should be changed to "(0.6‰)." This error has been corrected, and this may be considered the authoritative version of record.